JOURNAL OF THEORETICAL
AND APPLIED MECHANICS
48, 1, pp. 191-205, Warsaw 2010

ANALYSIS OF CONTACT MIXING WITH BOUNDARY AND HYDRODYNAMIC FLUID FILMS CONSIDERING BOUNDARY SLIPPAGE

Yongbin Zhang
Zhejiang Jinlei Electronic and Mechanical Co., Zhejiang Province, P.R. China
e-mail: engmech1@sina.com

An analysis is presented for a micro-contact where boundary and hydrodynamic fluid films simultaneously occur considering boundary slippage appearance at the upper contact surface in the boundary film area. The contact is one-dimensional, composed of two parallel plane surfaces, which are respectively rough rigid with rectangular projection in profile and ideally smooth rigid. In the outlet zone of the contact a boundary film occurs, and in the inlet zone of the contact a conventional hydrodynamic fluid film emerges. In the boundary film area, the film slips at the upper contact surface due to the limited shear stress capacity of the film-contact interface, while the film does not slip at the lower contact surface due to the shear stress capacity of the film-contact interface, which is large enough. In the boundary film area, the viscosity and density of the film are varied across the film thickness due to the film-contact interactions, and their effective values are used in modelling which depends on the boundary film thickness. In the fluid film area, the film does not slip at either of the contact surfaces.

Key words: boundary film, nanometer-scale thin film, fluid film, boundary slippage

1. Introduction

In engineering applications, two solid surfaces often slide one against another. The contact between them usually needs to generate the load-carrying capacity with the ability of low friction and anti-wear. To achieve this requirement, the contact is usually lubricated with fluids. Since the solid contact surface is actually rough, when in carrying the load and fluid lubrication, the contact between two solid surfaces is actually usually quite mixed. The author pointed out that in a hydrodynamic lubricated line or point, concentrated contacts, different contact regimes frequently simultaneously occur in different areas of the contact in modern industry (Zhang, 2004b, 2006b). Such contact regimes are conventional hydrodynamic lubricated contact, physical adsorbed boundary layer contact, chemical boundary layer contact and fresh solid material to material contact. Experiments and theories showed that these four contact regimes often simultaneously occur in the hydrodynamic concentrated contact with medium or heavy loads (Zhang, 2004a, 2006a,b; Begelinger and Gee de, 1974, 1976; Tabor, 1981).

In modelling of the hydrodynamic concentrated contact, however, the study goes backward to the experimental findings. It was pointed out that before 1990s the theoretical modelling of the hydrodynamic concentrated contact belongs to the classical modelling (Zhang, 2006b). In that modelling, although the contact surfaces were considered as rough, the whole contact between the two surfaces were treated as the conventional hydrodynamic lubricated contact, where the fluid film is relatively thick, see for example Goglia *et al.* (1984), Lubrecht *et al.* (1988). The theoretical modelling of the hydrodynamic concentrated contact at the end of the last century and in the begining of this century belongs to the modern modelling (Zhang, 2006b). In that modelling, the whole contact of the two surfaces is considered as consisted of different contact parts where different contact regimes respectively occur. These contact regimes may be the conventional hydrodynamic lubricated contact and surface asperity to asperity contact, see for example Jiang *et al.* (1999), Holmes *et al.* (2003). They may be also the conventional hydrodynamic lubricated contact and physical adsorbed boundary layer contact, see Zhang (2004a), Zhang *et al.* (2003), Zhang and Lu (2003). It was pointed out that in the future modelling of the hydrodynamic concentrated contact, conventional hydrodynamic lubricated contact, physical adsorbed boundary layer contact, chemical boundary layer contact and fresh solid material to material contact may need to be simultaneously considered and treated as occurring in different contact parts depending on the operating condition (Zhang, 2006b). In the recent modelling of the hydrodynamic contact, conventional hydrodynamic lubricated contact, physical adsorbed boundary layer contact and direct surface asperity to asperity contact between two surfaces were simultaneously considered and treated as occurring in different parts of the contact depending on the film thickness (Zhang, 2007a,b,c). It is a more advanced modelling of the contact. As that modelling showed, it is admitted that the physical adsorbed boundary layer contact and direct surface asperity to asperity contact both actually occur in micro-contact areas with a very small contact width, which are irregularly and discretely distributed in the realistic hydrodynamic contact.

The boundary slippage is a phenomenon occurring in the hydrodynamic contact when the film-contact interfacial shear stress exceeds the shear strength of the film-contact interface. Experiments (Bonaccurso *et al.*, 2003; Pit *et al.*, 2000; Craig *et al.*, 2001; Zhu and Granick, 2001) and molecular dynamics simulations (Thompson and Troian, 1997; Sun and Ebner, 1992) showed that the film-contact interfacial slippage can actually occur in a practical hydrodynamic contact not only of non-wetting or partially wetting systems but also of completely wetting systems due to the weak interaction strength and, then, the low shear strength of the film-contact interface. Experiments and molecular dynamics simulations showed that in micro-contact with boundary films the slippage at the film-contact interface needs to be considered in developing its load-carrying capacity theory. By molecular dynamics simulation, Thompson and Troian (1997) showed that in the micro-contact with boundary films, the boundary condition at the film-contact interface should be generally considered as slippage. They showed that this boundary slippage is a result of inefficient momentum transfer at the film-contact interface. It was determined by the interaction strength between the contact and the film. It was experimentally shown by Zhu and Granick (2001) that the film-contact interfacial slippage reduces the load-carrying capacity of boundary films in the micro-contact. Craig *et al.* (2001) experimentally found the slippage at the film-contact interface in the micro-contact with boundary films by using the Atomistic Force Microscope measurement. They found that the degree of the film-contact interfacial slippage in the micro-contact is increased with both contact surface speed and film viscosity. Sun and Ebner (1992), Cieplak *et al.* (2001) and Cheikh and Koper (2003) also observed the slippage occurring at the film-contact interface in the general micro-contact with boundary films, respectively by molecular dynamics simulation and experiments. They all found that the film-contact interfacial slippage is determined by the interaction strength between the contact and the film. It is generally agreed that a weak adhesion strength between the contact and the film or a repulsive wall yield film-contact interfacial slippage, while a strong film-contact attraction gives no slippage at the film-contact interface.

The present paper analytically investigates the boundary slippage effect in the micro-contact mixing with boundary and hydrodynamic fluid films considering the film-contact interfacial slippage in the boundary film area. The contact is one-dimensional, formed by two parallel rigid plane surfaces. The upper contact surface is rough with rectangular ridges in profile and the lower contact surface is ideally smooth. The boundary film is formed between the ridge of the upper contact surface and the lower contact surface. The fluid film is formed between the dent of the upper contact surface and the lower contact surface. The analytical approach proposed by the author and his colleagues (Zhang, 2006c,d; Zhang *et al.*, 2003) is used for the boundary film, and conventional hydrodynamic analysis is used for the fluid film.

2. Contact model

The micro-contact studied in the present paper is one-dimensional and isothermal, formed between two parallel rigid plane surfaces. The upper contact surface is stationary and rough with rectangular ridges in profile. The lower contact surface is moving and ideally smooth. In the micro-contact, the boundary film occurs in the outlet zone and the hydrodynamic fluid film occurs in the inlet zone. In the boundary film area, the film slips at the upper contact surface due to the limited shear stress capacity of the film-contact interface, and it does not slip at the lower contact surface due to the shear stress capacity of the film-contact interface, which is large enough. The viscosity and density properties of the boundary film are considered. In the fluid film area, the film does not slip at either of the contact surfaces. The fluid is entrained from the fluid film area into the boundary film area.

Figure 1 shows the profile of this micro-contact. In the figure, h_b is the boundary film thickness, h_a is the hydrodynamic fluid film thickness, l_a is the width of the fluid film area, l_b is the width of the boundary film area, and u is the speed of the lower contact surface.

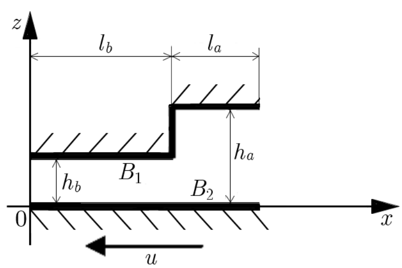

Fig. 1. Simulated micro-contact; B_1 – boundary film area, B_2 – hydrodynamic fluid film area

3. Analysis

The analysis of the pressures and carried loads of the micro-contact shown in Fig. 1 are respectively made with and without slippage assumed at the upper contact surface in the boundary film area, i.e. the B_1 sub-zone. The analyses are based on the following assumptions:

(a) The flow is one-dimensional;

(b) The pressure across the film thickness is constant;

(c) The film inertia is negligible;

(d) The operating condition is steady-state.

These assumptions are usually realistic. Also, in the present analysis, the boundary film shear elastic modulus effect is neglected (Zhang, 2009a,b).

The used coordinates are shown in Fig. 1. The pressure boundary conditions of the micro-contact are

$$p|_{x=0} = 0 \qquad\qquad p|_{x=(l_b+l_a)} = 0 \tag{3.1}$$

3.1. No slippage at the upper contact surface in the boundary film area

The approach proposed by the author and his colleagues (Zhang, 2006c; Zhang *et al.*, 2003) is used to analyse the boundary film behaviour in the B_1 sub-zone in Fig. 1. The approach needs to incorporate both the molecular dynamics effect and the non-continuum effect of the boundary film. The boundary film non-continuum effect is described by the flow factor approach (Zhang and Lu, 2005; Zhang, 2006d) which incorporates the boundary film discontinuity and inhomogeneity effects across the film thickness. According to the previous simulation for the same contact, the value of the flow factor θ_v depicting the boundary film non-continuum effect is very small (no more than 1.01) (Zhang, 2008). It means that in the present analysis, the value of θ_v can be taken as unity and the boundary film non-continuum effect is negligible. The boundary film molecular dynamics effect is described by the following equivalent continuum rheological model (Zhang, 2004a,b; Zhang *et al.*, 2003)

$$\begin{aligned} \dot{\gamma} &= \frac{\tau}{\eta_{bf}^{eff}(p, h_b)} && \text{for} \quad |\tau| < \tau_l \\ \tau &= \operatorname{sgn}(\dot{\gamma})\tau_l && \text{for} \quad |\tau| \geqslant \tau_l \end{aligned} \tag{3.2}$$

where τ is the shear stress, $\dot{\gamma}$ – shear strain rate, η_{bf}^{eff} – boundary film effective viscosity, and τ_l – limiting shear stress. In the present case, within the boundary film and at the two contact surfaces $\tau_l = +\infty$. The model assumes that slippage does not occur either within the boundary film or at the two contact surfaces.

The boundary film viscosity is predicted by the following equation (Zhang *et al.*, 2003; Zhang and Lu, 2003)

$$\eta_{bf}^{eff}(h_b) = C_y(h_b)\eta_c \qquad \text{for} \quad 0 < \frac{h_b}{h_{cr,bf}} < 1 \tag{3.3}$$

where η_c is constant representing the average viscosity of the continuum film at the pressure of the boundary film area, $h_{cr,bf}$ is the critical boundary film thickness, and C_y is expressed as

$$C_y(h_b) = a_0 + a_1\Big(\frac{h_b}{h_{cr,bf}}\Big)^{-1} + a_2\Big(\frac{h_b}{h_{cr,bf}}\Big)^{-2} \tag{3.4}$$

where a_0, a_1 and a_2 are constants.

The boundary film density is expressed as (Zhang *et al.*, 2003; Zhang and Lu, 2003)

$$\rho_{bf}^{eff}(h_b) = C_q(h_b)\rho_c \qquad \text{for} \quad 0 < \frac{h_b}{h_{cr,bf}} < 1 \tag{3.5}$$

where ρ_c is constant representing the average density of the continuum film at the pressure of the boundary film area, and C_q is expressed as

$$C_q(h_b) = g_0 + g_1\frac{h_b}{h_{cr,bf}} + g_2\Big(\frac{h_b}{h_{cr,bf}}\Big)^2 + g_3\Big(\frac{h_b}{h_{cr,bf}}\Big)^3 \tag{3.6}$$

where g_0, g_1, g_2 and g_3 are constants.

The Reynolds equation in the boundary film area is

$$q_m = -\frac{uh_b\rho_{bf}^{eff}}{2} - \frac{\rho_{bf}^{eff}h_b^3}{12\eta_{bf}^{eff}}\frac{dp}{dx} \tag{3.7}$$

where q_m is the mass flow through the contact.

Define

$$\lambda_{b,bf} = -12\Big(q_m + \frac{1}{2}uh_b\rho_{bf}^{eff}\Big)\eta_c\frac{C_y}{\rho_{bf}^{eff}h_b^3}$$

Solving Eq. (3.7) by using the boundary condition expressed by Eq. (3.1) gives the pressure in the boundary film area as follows

$$p = \lambda_{b,bf}x \tag{3.8}$$

The Reynolds equation in the B_2 sub-zone in Fig. 1 is

$$q_m = -\frac{1}{2}\rho_c u h_a - \frac{\rho_c h_a^3}{12\eta_c}\frac{dp}{dx} \tag{3.9}$$

Define

$$\lambda_{a,\rho} = -12\eta_c \frac{1}{h_a^3}\Big(\frac{q_m}{\rho_c} + \frac{1}{2}uh_a\Big)$$

Solving Eq. (3.9) by using the boundary condition expressed by Eq. (3.1) gives the pressure in the B_2 sub-zone as follows

$$p = \lambda_{a,\rho}(x - l_a - l_b) \tag{3.10}$$

From the constraint condition that the pressure at $x = l_b$ in Fig. 1 is continuous, the mass flow through the contact q_m is obtained by solving the constraint equation on the pressure at $x = l_b$ as follows

$$q_m = -\frac{u\rho_c\phi_2(h_b + h_a\phi_1)}{2(1 + \phi_1\phi_2)} \tag{3.11}$$

where $\phi_1 = r_l/(r_h^3 C_y)$, $\phi_2 = C_q$. Here $r_l = l_a/l_b$ and $r_h = h_a/h_b$.

The carried load (per unit contact length) by the micro-contact is derived as

$$w_1 = \frac{\lambda_{b,bf}l_b^2 - \lambda_{a,\rho}l_a^2}{2} \tag{3.12}$$

The pressure at $x = l_b$ is

$$p_{no-slip}|_{x=l_b} = \lambda_{b,bf}l_b \tag{3.13}$$

3.2. Slippage at the upper contact surface in the boundary film area

In this case, the boundary film non-continuum effect is negligible due to the value of θ_v approaching unity. The boundary film molecular dynamics effect is still described by Eq. (3.2). For this case, in Eq. (3.2), within the boundary film and at the film-lower contact surface interface $\tau_l = +\infty$, while at the film-upper contact surface interface $\tau_l = \tau_s$. Here, τ_s is the shear strength of the film-upper contact surface interface. The model assumes that slippage does not occur either within the boundary film or at the film-lower contact surface interface, but can occur at the film-upper contact surface interface if the magnitude of the shear stress at the film-upper contact surface interface exceeds the value of τ_s.

The shear strength τ_s of the film-upper contact surface interface is predicted by the following equation (Zhang *et al.*, 2003; Zhang and Lu, 2003)

$$\tau_s(h_b) = C_{taol}^i(h_b)\tau_{s,c} \qquad \text{for} \qquad \beta_0 \leqslant \frac{h_b}{h_{cr,bf}} < 1 \tag{3.14}$$

where $\tau_{s,c}$ is constant representing the average shear strength of the continuum film-upper contact surface interface at the pressure of the boundary film area, and C_{taol}^{i} is expressed as

$$C_{taol}^{i}(h_b) = d_0^i + d_1^i \Big(\frac{h_b}{h_{cr,bf}}\Big)^{-1} + d_2^i \Big(\frac{h_b}{h_{cr,bf}}\Big)^{-2} \tag{3.15}$$

where d_0^i, d_1^i and d_2^i are constants.

The Reynolds equation for the boundary film area is

$$q_m = B_0 + B_1 \frac{dp}{dx} \tag{3.16}$$

where q_m is the mass flow through the contact and

$$B_0 = \frac{\rho_{bf}^{eff} \tau_s h_b^2}{2\eta_{bf}^{eff}} - \rho_{bf}^{eff} u h_b \qquad B_1 = -\frac{\rho_{bf}^{eff} h_b^3}{2\eta_{bf}^{eff}}$$

The solution of Eq. (3.16) is

$$p = \frac{q_m - B_0}{B_1} x + c \tag{3.17}$$

From the boundary condition $p(0) = 0$, it is solved that $c = 0$. The pressure in the boundary film area is then expressed as

$$p = \frac{q_m - B_0}{B_1} x \tag{3.18}$$

At $x = l_b$, the film pressure is

$$p_{slip}|_{x=l_b} = \frac{(q_m - B_0) l_b}{B_1} \tag{3.19}$$

According to Section 3.1, it is solved from the fluid film area that at $x = l_b$ the film pressure is $p_{slip}|_{x=l_b} = -\lambda_{a,\rho} l_a$. It is then equated that

$$\frac{q_m - B_0}{B_1} l_b = -\lambda_{a,\rho} l_a \tag{3.20}$$

It is solved from Eq. (3.20) that

$$q_m = \frac{u h_a \rho_c \Big(6 r_l + 2 C_y r_h^2 - \frac{\tau_s h_a r_h}{u \eta_c}\Big)}{-12 r_l - \frac{2 C_y r_h^3}{C_q}} \tag{3.21}$$

The load per unit contact length carried by the micro-contact is

$$w_2 = \frac{q_m - B_0}{2B_1} l_b^2 - \frac{1}{2} \lambda_{a,\rho} l_a^2 \tag{3.22}$$

3.3. Performance parameters of the contact

Define the relative reduction of the carried load of the contact due to the boundary slippage as

$$r_w = \frac{w_1 - w_2}{w_1} \tag{3.23}$$

The value of r_w can reflect the influence of the boundary slippage on the load-carrying capacity of the contact.

Define the relative reduction of the pressure at $x = l_b$ due to the boundary slippage as

$$r_p = \frac{p_{no-slip}|_{x=l_b} - p_{slip}|_{x=l_b}}{p_{no-slip}|_{x=l_b}} \tag{3.24}$$

The value of r_p can reflect the influence of the boundary slippage on the local pressure in the contact.

Define the relative increase of the mass flow through the contact due to the boundary slippage as

$$I_q = \frac{|q_{m,slip}| - |q_{m,no-slip}|}{|q_{m,no-slip}|} \tag{3.25}$$

where $q_{m,no-slip}$ is calculated from Eq. (3.11) and $q_{m,slip}$ is calculated from Eq. (3.21).

4. Results

The values of r_w, r_p and I_q are respectively calculated for two cases. Case 1 represents the heavy load and high sliding speed operating condition. Case 2 represents the light load and low sliding speed operating condition. The operational parameter values for these two cases are respectively listed as follows:

Case 1: $\eta_c = 4000\,\mathrm{Pa\,s}$, $u = 100\,\mathrm{m/s}$, $l_a + l_b = 1\,\mu\mathrm{m}$, $h_{cr,bf} = 20\,\mathrm{nm}$, $h_a - h_b = 20\,\mathrm{nm}$, $r_l = 0.5$, $\rho_c = 960\,\mathrm{kg/m^3}$, $\tau_{s,c} = 1 \sim 100\,\mathrm{MPa}$.

Case 2: $\eta_c = 0.1\,\mathrm{Pa\,s}$, $u = 0.01\,\mathrm{m/s}$, $l_a + l_b = 1\,\mu\mathrm{m}$, $h_{cr,bf} = 20\,\mathrm{nm}$, $h_a - h_b = 20\,\mathrm{nm}$, $r_l = 0.5$, $\rho_c = 960\,\mathrm{kg/m^3}$, $r_h = 11$ ($h_b = 2\,\mathrm{nm}$).

These two cases have the same boundary film property parameter values shown in Table 1.

Table 1. Boundary film property parameter values

β_0	a_0	a_1	a_2	g_0	g_1
0.075	1.0822	−0.1758	0.0936	1.30	−1.0654
g_2	g_3	d_0^i	d_1^i	d_2^i	
1.3361	−0.571	0.9726	0.0261	$1.3158 \cdot 10^{-3}$	

4.1. Case 1

It is found that for Case 1 the values of r_w, r_p and I_q are not dependent on the interfacial shear strength $\tau_{s,c}$ but obviously depend on the boundary film thickness h_b, when the value of $\tau_{s,c}$ ranges between 1 MPa and 100 MPa. This may be a common result for the heavy load and high sliding speed condition. It may be drawn that in the heavy load and high sliding speed condition the reductions of the carried load and the local pressure of the contact and the increase of the mass flow through the contact due to the boundary slippage in the boundary film area are practically not determined by the boundary film-contact interfacial shear strength but determined by the boundary film thickness.

Figure 2 plots the values of r_w, r_p and I_q against the dimensionless boundary film thickness obtained for Case 1. The values of r_w and r_p are nearly linearly increased with the increase of the boundary film thickness h_b and strongly influenced by the boundary film thickness. The value of r_w appears considerable. It means that the boundary slippage considerably reduces the load-carrying capacity of the micro-contact.

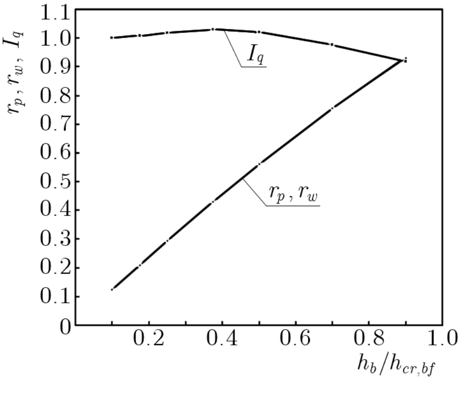

Fig. 2. Plots of the values of r_w, r_p and I_q against the dimensionless boundary film thickness obtained for Case 1

Researches may also care about the value of r_p at a small boundary film thickness. It is shown in Fig. 2 that the value of r_p is increased from 0.12 to 0.3 when the boundary film thickness h_b is increased from 2 nm to 5 nm. It is found that when the boundary film thickness is below 5 nm, the boundary slippage occurring in the boundary film area can cause considerable reductions of the local pressure in the micro-contact. This reduction may be able to considerably influence the contact surface elastic deformations and then the local film thickness when the contact surfaces are elastic and the boundary film thickness is on the film molecule size scale. Figure 2 suggests that when the boundary film thickness is below 5 nm and the boundary film is considered in the mixed contact modelling, the model should also consider the boundary film-contact interfacial slippage, probably occurring in the contact and influencing the local film thickness.

Figure 2 shows that the boundary slippage in the boundary film area causes the mass flow through the contact increased nearly one times in the condition of heavy load and high sliding speed for all boundary film thicknesses. At a small boundary film thickness, this increase is more significant.

4.2. Case 2

Figure 3 plots values of r_w, r_p and I_q against the interfacial shear strength $\tau_{s,c}$ obtained for Case 2. It is found that in the condition of a light load and low sliding speed, the values of r_w, r_p and I_q strongly depend on the boundary film-contact interfacial shear strength. These values are shown to be linearly increased with the reduction of the boundary film-contact interfacial shear strength. In the condition of the light load and low sliding speed, the boundary film interfacial slippage can also considerably reduce the load-carrying capacity of the micro-contact. Although the values of r_p are shown to be small, the local pressure reductions under these r_p values due to the boundary slippage are usually able to considerably influence the local film thickness by changing the local contact surface elastic deformations when the contact surfaces are elastic and the boundary film thickness is on the film molecule size scale. In the mixed contact modelling, for the condition of the light load and low sliding speed, when the boundary film thickness is below 5 nm and the boundary film is considered, the boundary film-contact interfacial shear strength and the boundary film-contact interfacial slippage need to be considered. For the light load and low sliding speed condition, the reduction of the boundary film-contact interfacial shear strength is shown to significantly increase the mass flow through the contact.

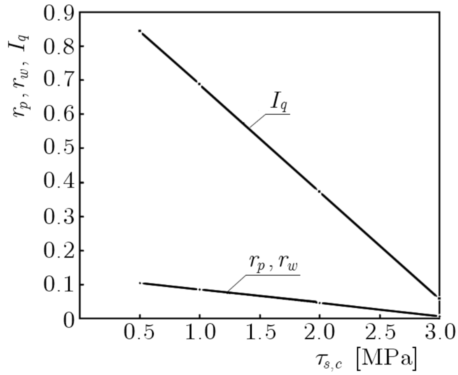

Fig. 3. Plots of the values of r_w, r_p and I_q against the interfacial shear strength $\tau_{s,c}$ obtained for Case 2

5. Conclusions

The present paper analytically investigates the effect of the boundary film-contact interfacial slippage on the local pressure, carried load and mass flow of the micro-contact. The contact is a mixed contact. In its outlet zone there occurs a physical adsorbed boundary layer, and in its inlet zone a conventional hydrodynamic fluid film. The contact is formed between two parallel rigid plane surfaces. The upper contact surface is rough with rectangular projection. The lower contact surface is ideally smooth. The boundary film is assumed to slip at the upper contact surface but not slip at the lower contact surface. It is also assumed not to slip within the film. The conventional hydrodynamic fluid film is assumed not to slip at either of the contact surfaces.

It is found that when the boundary film thickness is below 5 nm, the boundary slippage occurring in the boundary film area can cause considerable reductions of the local pressure in the micro-contact. This reduction may be able to considerably influence the contact surface elastic deformations and, then, the local film thickness when the contact surfaces are elastic and the boundary film thickness is on the film molecule size scale. It is suggested that when the boundary film thickness is below 5 nm and the boundary film is considered in the mixed contact modelling, the model should also consider the boundary film-contact interfacial shear strength and the boundary film-contact interfacial slippage, which probably occurs in the contact and influences the local film thickness.

Project support: Natural Science Foundation of Jiangsu Province, China (BK2008189).

References

1. Begelinger A., Gee de A.W.J., 1974, Thin film lubrication of sliding point contacts of AISI 52100 steel, *Wear*, **28**, 103-114

2. Begelinger A., Gee de A.W.J., 1976, On the mechanism of lubricant film failure in sliding concentrated steel contacts, *ASME J. Lubr. Techn.*, **98**, 575-579

3. Bonaccurso E., Butt H.J., Craig V.S.J., 2003, Surface roughness and hydrodynamic boundary slip of a Newtonian fluid in a completely wetting system, *Phys. Rev. Lett.*, **90**, 144501

4. Cheikh C., Koper G., 2003, Stick-slip transition at the nanometer scale, *Phys. Rev. Lett.*, **91**, 156102

5. Cieplak M., Koplik J., Banavar J.R., 2001, Boundary conditions at a fluid-solid interface, *Phys. Rev. Lett.*, **86**, 803-806

6. Craig V.S.J., Neto C., Williams D.R.M., 2001, Shear-dependent boundary slip in an aqueous Newtonian liquid, *Phys. Rev. Lett.*, **87**, 054504

7. Goglia P.R., Conry T.F., Cusano C., 1984, The effects of surface irregularities on the elastohydrodynamic lubrication of sliding line contacts: Part I – Single irregularities, *ASME J. Trib.*, **106**, 104-112

8. Holmes M., Evans H.P., Hughs T.G., Snidle R.W., 2003, Transient elastohydrodynamic point contact analysis using a new coupled differential deflection method. Part 2: results, *Proc. Instn. Mech. Engrs. Part J: J. Eng. Trib.*, **217**, 305-321

9. Jiang X., Hua D.Y., Cheng H.S., Ai X., Lee S.C., 1999, Mixed elastohydrodynamic lubrication model with asperity contact, *ASME J. Trib.*, **121**, 481-491

10. Lubrecht A.A., Napel W.E., Bosma R., 1988, The influence of longitudinal and transverse roughness on the elastohydrodynamic lubrication of circular contacts, *ASME J. Trib.*, **110**, 421-426

11. Pit R., Hervet H., Leger L., 2000, Direct experimental evidence of slip in hexadecane: solid interfaces, *Phys. Rev. Lett.*, **85**, 980-983

12. Sun M., Ebner C., 1992, Molecular dynamics study of flow at a fluid-wall interface, *Phys. Rev. Lett.*, **69**, 3491-3494

13. Tabor B.J., 1981, Failure of thin film lubrication-An expedient for the characterization of lubricants, *ASME J. Lubric. Techn.*, **103**, 497-501

14. Thompson P.A., Troian S.M., 1997, A general boundary condition for liquid flow at solid surfaces, *Nature*, **389**, 360-362

15. Zhang Y.B., 2004a, Mixed rheologies in elastohydrodynamic lubrication, *Industr. Lubric. Trib.*, **56**, 88-106

16. Zhang Y.B., 2004b, Modeling of elastohydrodynamic lubrication with molecularly thin lubricating films, *J. Balkan Tribol. Assoc.*, **10**, 394-421

17. Zhang Y.B., 2006a, Contact-fluid interfacial shear strength and its critical importance in elastohydrodynamic lubrication, *Industr. Lubric. Trib.*, **58**, 4-14

18. Zhang Y.B., 2006b, Contact-fluid interfacial slippage in hydrodynamic lubricated contacts, *J. Mol. Liq.*, **128**, 99-104

19. Zhang Y.B., 2006c, Flow factor approach to molecularly thin hydrodynamic film lubrication, *J. Mol. Liq.*, **128**, 60-64

20. Zhang Y.B., 2006d, Flow factor of non-continuum fluids in one-dimensional contact, *Industr. Lubric. Trib.*, **58**, 151-169

21. Zhang Y.B., 2007a, Study of an engineering mixed contact: Part I – Theoretical analysis, *J. Applied Sci.*, **7**, 1249-1259

22. Zhang Y.B., 2007b, Study of an engineering mixed contact: Part II – Results for isosceles triangle surface ridges, *J. Applied Sci.*, **7**, 1351-1361

23. Zhang Y.B., 2007c, Study of an engineering mixed contact: Part III – Results for isosceles truncated triangle surface ridges, *J. Applied Sci.*, **7**, 1467-1474

24. Zhang Y.B., 2009a, Boundary film shear elastic modulus effect in hydrodynamic contact. Part I: theoretical analysis and typical solution, *Theor. Comp. Fluid Dyn.*, **23**, 239-254

25. Zhang Y.B., 2009a, Boundary film shear elastic modulus effect in hydrodynamic contact. Part II: influence of operational parameters, *Theor. Comp. Fluid Dyn.*, **23**, 255-269

26. Zhang Y.B., Lu G.S., 2003, Model of elastohydrodynamic lubrication with molecularly thin lubricating films: Part II – Results for an exemplary lubrication, *Int. J. Fluid Mech. Res.*, **30**, 558-571

27. Zhang Y.B., Lu G.S., 2005, Flow factor for molecularly thin fluid films in one-dimensional flow due to fluid discontinuity, *J. Mol. Liq.*, **116**, 43-50

28. Zhang Y.B., Tang K., Lu G.S., 2003, Model of elastohydrodynamic lubrication with molecularly thin lubricating films: Part I – Development of analysis, *Int. J. Fluid Mech. Res.*, **30**, 542-557

29. Zhu Y.X., Granick S., 2001, Rate-dependent slip of Newtonian liquid at smooth surfaces, *Phys. Rev. Lett.*, **87**, 096105

Analiza kontaktu mieszanego z uwzględnieniem poślizgu brzegowego w strefie hydrodynamicznego filmu

Streszczeie

Analiza zaprezentowana w pracy dotyczy zagadnienia mikro-kontaktu w strefie jednoczesnego występowania brzegowego i hydrodynamicznego filmu płynu z możliwością poślizgu w strefie brzegowej na górnej powierzchni kontaktu. Rozważany kontakt jest jednowymiarowy i odnosi się do dwóch równoległych płaskich powierzchni, z których jedna jest sztywna i szorstka w przekroju prostopadłym, a druga tak samo sztywna lecz idealnie gładka. W obszarze wyjścia ze strefy kontaktu pojawia się brzegowy film płynu, natomiast w strefie wejścia konwencjonalny film hydrodynamiczny. W strefie brzegowej film ulega poślizgowi na górnej powierzchni wskutek ograniczonej zdolności przenoszenia naprężeń stycznych pomiędzy płynem a ścianką, natomiast na powierzchni dolnej poślizg nie występuje. W strefie brzegowej filmu jego lepkość i gęstość zmienia się wzdłuż grubości wskutek interakcji płynu z powierzchnią. Efektywne wartości użyte w modelowaniu kontaktu zależą od grubości filmu brzegowego. W regularnej strefie film nie ulega poślizgowi na żadnej z omawianych powierzchni.

Manuscript received May 7, 2009; accepted for print July 23, 2009